

A nonorthogonal state-interaction approach for matrix product state wave functions

Stefan Knecht,^{1, a)} Sebastian Keller,¹ Jochen Autschbach,² and Markus Reiher¹

¹⁾*ETH Zürich, Laboratorium für Physikalische Chemie, Vladimir-Prelog-Weg 2, 8093 Zürich, Switzerland*

²⁾*University at Buffalo, State University of New York, Department of Chemistry, New York 14260-3000, United States of America*

We present a state-interaction approach for matrix product state (MPS) wave functions in a nonorthogonal molecular orbital basis. Our approach allows us to calculate for example transition and spin-orbit coupling matrix elements between arbitrary electronic states provided that they share the same one-electron basis functions and active orbital space, respectively. The key element is the transformation of the MPS wave functions of different states from a nonorthogonal to a biorthonormal molecular orbital basis representation exploiting a sequence of non-unitary transformations following a proposal by Malmqvist (*Int. J. Quantum Chem.* **30**, 479 (1986)). This is well-known for traditional wave-function parametrizations but has not yet been exploited for MPS wave functions.

^{a)}Electronic mail: stefan.knecht@phys.chem.ethz.ch

I. INTRODUCTION

The calculation of electronic and vibronic transition matrix elements between electronic states of the same or different spin and/or spatial symmetry is a ubiquitous task in the modeling of photochemical and photophysical processes. Prime examples include the modeling of non-adiabatic dynamics processes^{1,2} as well as light-induced excited spin-state trapping phenomena^{3,4}. The theoretical description of these processes builds upon the calculation of intersystem crossing rates⁵ which, besides electronic and vibronic coupling elements, requires the evaluation of spin-orbit (SO) coupling (SOC) matrix elements. Similarly, calculating magnetic properties⁶ such as molecular g-factors and electron-nucleus hyperfine coupling, which are central parameters in electron paramagnetic resonance (EPR) spectroscopy, requires spin-orbit coupled wave functions^{7,8}. To this end, correlated two- and four-component *ab initio* wave function^{9–12}, and density functional theory approaches^{13–15}. In the present study we focus on EPR g-tensors for testing purposes, but it should be noted that the underlying novel method of gaining access to wave functions that include the effects from SOC has a vast range of applications.

While it is possible to treat SOC variationally, a considerable number of two-step correlated wave function approaches for the calculation of molecular g-factors were developed over the past decades (see, for example, Refs. 9,16–23 and literature citations in these works and in Refs. 8–11,13–15). In these schemes, the calculation of a number of non- or scalar-relativistic many-particle spin-free states that are eigenfunctions of the spin-squared operator S^2 , is decoupled from a subsequent perturbative or variational mixing of the latter through the SO coupling operator to obtain SO coupled many-electron wave functions (e.g. by diagonalization “state-interaction”). It is straightforward to calculate properties such as g-factors in the basis of the eigenstates of the SO operator subsequently. Appealing features of the two-step approaches are that valuable insight into contributions of each (ground or excited) spin-state to the g-tensor is gained, and that the underlying wave function basis is spin-adapted. The price to pay is the need to calculate a sufficient number of spin-free states to interact, which can amount up to several hundred states to achieve convergence for (heavy-element containing) molecules where electron correlation and spin-orbit coupling contributions can be of similar order of magnitude.

Open shell electronic structures are often governed by strong electron correlation effects.

In this context, multiconfigurational methods are the preferred methods of choice^{24,25} which typically split electron correlation into a static and a dynamic contribution. However, such a separation requires careful attention²⁶. A well-established approach to handle static correlation is the complete active space self-consistent field (CASSCF) ansatz²⁷ which requires to select a tailored number of (partially occupied) active orbitals. The selection of active orbitals is a tedious procedure but can be automatized^{26,28}. Since the computational cost of traditional CASSCF scales exponentially with the number of active orbitals and electrons, tractable active orbital spaces are presently limited to about 18 electrons in 18 orbitals²⁹. These limitations can be overcome by resorting to the density matrix renormalization group (DMRG) approach³⁰⁻³³ in quantum chemistry³⁴⁻⁴⁴ which, in combination with a self-consistent-field orbital optimization ansatz (DMRG-SCF)^{45,46}, is capable of approximating CASSCF wave functions to chemical accuracy with merely a polynomial scaling. DMRG-SCF therefore allows to handle much larger active orbital spaces that can boldly surpass the CASSCF limit. To account in addition for spin-orbit coupling in a DMRG framework, variational SO approaches⁴⁷ as well as two-step approaches^{22,23} based on spin-free DMRG wave functions have been reported recently.

In this work, we present a generalized state-interaction approach for *nonorthogonal* spin-free matrix product state (MPS) wave functions which enables the evaluation of arbitrary one- and two-particle transition matrix elements as well as SO coupling matrix elements. Diagonalization of the SO Hamiltonian matrix, for instance, yields spin-orbit coupled wave functions as linear combinations of the uncoupled, spin-pure MPS states. The latter can (but do not have to) be obtained as results from one or several DMRG-SCF orbital optimization calculations. This allows for utmost flexibility in the individual DMRG-SCF steps as each state-specific or spin-specific state-averaged orbital optimization is given the possibility to reflect potential relative differences in open-shell occupancies. For example, transition metal as well as lanthanide and actinide complexes often exhibit different *s*- and *d*-occupations (transition metals) and *s*-, *d*- and *f*-occupations (lanthanides/actinides) in ground- and electronically excited electronic states of various spin symmetries.

However, a set of wave functions that were optimized individually generally implies mutual nonorthogonality of the respective MO bases. Moreover, the MO bases may neither be orthogonal to each other nor non-interacting which can, e.g., strongly affect the calculation of transition moments between such electronic states⁴⁸. As first shown in a landmark paper

by Malmqvist⁴⁹, an elegant approach for the calculation of matrix elements and transition density matrices is the transformation to a biorthonormal basis for the bra and ket orbital basis of the respective wave functions. A change of the MO basis to a biorthonormal orbital basis necessitates, however, not only to transform all one- and two-electron integrals but to also “counter-rotate” the configuration basis of the wave function. For configuration-interaction (CI)-type expansions, the rotations and counter-rotations can be achieved by a sequence of single-orbital transformations^{49,50} that require only one-electron operations. Subsequently, standard second-quantization algebra can be exploited for the evaluation of overlap matrix elements as well as arbitrary one- and two-particle matrix elements between the states in the biorthonormal basis. In a recent work, Olsen⁵¹ exploited the potential of the biorthonormal approach further to devise an efficient algorithm for CI and orbital optimization schemes based on nonorthogonal orbitals. In contrast to previous nonorthogonal CI approaches (cf. Ref. 52), this newly proposed algorithm⁵¹ requires only the calculation of one- and two-particle reduced density matrices.

In this paper, we derive the working equations to calculate one- and two-particle matrix elements between MPS wave functions that may be originally expressed in different, mutually nonorthogonal molecular orbital bases. Following the work of Malmqvist⁴⁹, the central element of our algorithm is the transformation of the bra and ket MPS wave functions to a biorthonormal basis representation. It is important to stress that the latter transformation is not needed if the MPS wave functions that are considered for state interaction share a common MO basis (cf. Refs. 22 and 23). After solving a generalized eigenvalue equation of the form

$$\mathbf{H}\mathbf{c} = E\mathbf{S}\mathbf{c} , \tag{1}$$

with the Hamiltonian matrix \mathbf{H} expressed in the basis of the DMRG-SCF wave functions and the overlap matrix \mathbf{S} we obtain a set of fully orthogonal and non-interacting states as linear combinations of the DMRG-SCF wave functions with the expansion coefficients given by \mathbf{c} .

Since Malmqvist’s approach⁴⁹ assumes either a full CI expansion or, in general terms, a wave function expansion that is closed under de-excitation^{53–55} we probe the closedness of our MPS wave function transformation by systematically increasing its numerical accuracy for a given active orbital space.

In Section II we briefly discuss the theoretical framework for a second quantization formal-

ism based on nonorthogonal orbitals. In Section III we introduce an algorithm to calculate expectation values for nonorthogonal wave functions in an MPS and matrix-product operator (MPO) representation of the wave function and operators^{56,57}, respectively, based on a nonunitary orbital transformation and demonstrate in Section IV how the latter can be exploited for a nonorthogonal MPS state-interaction (MPS-SI) *ansatz*. Numerical examples for the calculation of g-factors for f^1 - and f^2 -type actinide complexes are presented in Section V.

II. SECOND QUANTIZATION FOR NONORTHOGONAL ORBITALS

In this section, we briefly summarize the second quantization formalism for nonorthogonal orbitals^{50,51,58,59}. In what follows, all quantities expressed in an orthonormal orbital basis are denoted by a tilde, those in the biorthonormal basis will be labeled by a bar whereas quantities with no extra label refer to a nonorthogonal orbital basis.

Assuming an arbitrary set of N (linearly independent) MOs $\varphi = \{\varphi_p\}$ with the general overlap matrix $\mathbf{S} = \{S_{pq}\}$

$$S_{pq} = \langle \varphi_p | \varphi_q \rangle = \int d\mathbf{r} \varphi_p^*(\mathbf{r})\varphi_q(\mathbf{r}) , \quad (2)$$

we can define a new set of orbitals $\tilde{\varphi} = \{\tilde{\varphi}_p\}$ that form an orthonormal basis by applying a Löwdin symmetric orthogonalization⁶⁰

$$\tilde{\varphi} = \varphi \mathbf{S}^{-1/2} . \quad (3)$$

For an element of the overlap matrix in the new basis then holds

$$\tilde{S}_{pq} = (\mathbf{S}^{-1/2\dagger} \mathbf{S} \mathbf{S}^{-1/2})_{pq} = \delta_{pq} , \quad (4)$$

and consequently the new orbital set $\{\tilde{\varphi}\}$ is orthonormal. The corresponding set of creation (annihilation) operators $\{\tilde{a}_{p\sigma}^\dagger\}$ ($\{\tilde{a}_{p\sigma}\}$) for spin orbitals, $\tilde{\varphi}_p(\mathbf{r})\sigma(m_s)$, in the new basis is related to the set of creation (annihilation) operators $\{a_{p\sigma}^\dagger\}$ ($\{a_{p\sigma}\}$) for spin orbitals of the original (nonorthogonal) basis⁵⁹,

$$\tilde{a}_{p\sigma}^\dagger = \sum_q a_{q\sigma}^\dagger S_{qp}^{-1/2} , \quad (5)$$

$$\tilde{a}_{p\sigma} = \sum_q a_{q\sigma} S_{pq}^{-1/2} . \quad (6)$$

Note that the creation $\{\tilde{a}_{p\sigma}^\dagger\}$ and annihilation $\{\tilde{a}_{p\sigma}\}$ operators satisfy the well-known anti-commutation rules.

Expressing the creation (annihilation) operators of the nonorthogonal basis in terms of the operators defined in the orthonormal basis yields⁵⁹

$$a_{p\sigma}^\dagger = \sum_q \tilde{a}_{q\sigma}^\dagger S_{qp}^{1/2} , \quad (7)$$

$$a_{p\sigma} = \sum_q \tilde{a}_{q\sigma} S_{pq}^{1/2} . \quad (8)$$

Inserting Eq. (7) into the definition of the anticommutator, it is easy to verify that two creation operators in the nonorthogonal basis anticommute as it is the case in the orthonormal basis,

$$\{a_{p\sigma}^\dagger, a_{q\tau}^\dagger\} = \sum_{\substack{rs \\ \sigma\tau}} \{\tilde{a}_{r\sigma}^\dagger S_{rp}^{1/2}, \tilde{a}_{s\tau}^\dagger S_{sq}^{1/2}\} = \sum_{\substack{rs \\ \sigma\tau}} S_{rp}^{1/2} S_{sq}^{1/2} \underbrace{\{\tilde{a}_{r\sigma}^\dagger, \tilde{a}_{s\tau}^\dagger\}}_{=0} = 0 , \quad (9)$$

where we exploited in the second step the anticommutation of two creation operators for orthonormal spin orbitals. The same result holds for the anticommutation relation of two annihilation operators which is shown by Hermitian conjugation of Eq. (9). The anticommutator between a creation and annihilation operator reads

$$\{a_{p\sigma}^\dagger, a_{q\tau}\} = \sum_{\substack{rs \\ \sigma\tau}} \{\tilde{a}_{r\sigma}^\dagger S_{rp}^{1/2}, \tilde{a}_{s\tau} S_{qs}^{1/2}\} = \sum_{\substack{rs \\ \sigma\tau}} S_{rp}^{1/2} S_{qs}^{1/2} \underbrace{\{\tilde{a}_{r\sigma}^\dagger, \tilde{a}_{s\tau}\}}_{=\delta_{rs}\delta_{\sigma\tau}} = \sum_{\substack{r \\ \sigma\tau}} S_{qr}^{1/2} S_{rp}^{1/2} \delta_{\sigma\tau} = S_{qp} \delta_{\sigma\tau} . \quad (10)$$

Hence, whereas the anticommutator for a general pair $\tilde{a}_{p\sigma}^\dagger, \tilde{a}_{q\tau}^\dagger$ of creation- and annihilation operators reduces in the orthonormal orbital basis to

$$\{\tilde{a}_{p\sigma}^\dagger, \tilde{a}_{q\tau}\} = \delta_{pq} \delta_{\sigma\tau} , \quad (11)$$

it depends on the (in general non-vanishing) overlap matrix element S_{qp} in the nonorthogonal case.

As a consequence, the action of an annihilator $a_{q\sigma}$ on a given occupation number vector (ONV) $|\mathbf{k}\rangle$

$$|\mathbf{k}\rangle = \prod_{p=1}^L (a_{p\sigma}^\dagger)^{k_{p\sigma}} |\text{vac}\rangle = |k_1 k_2 \dots k_L\rangle , \quad (12)$$

with

$$k_{p\sigma} = \begin{cases} 1 & \text{if } \varphi_p(\mathbf{r})\sigma(m_s) \text{ occupied} \\ 0 & \text{if } \varphi_p(\mathbf{r})\sigma(m_s) \text{ unoccupied} \end{cases} \quad (13)$$

leads to a sum of ONVs⁵⁹

$$a_{q\sigma} |\mathbf{k}\rangle = \sum_p^L (-1)^{\left[\sum_{j=1}^{p-1} k_{j\sigma} \right]} S_{qp} k_{p\sigma} |k_1 k_2 \dots 0_p \dots k_L\rangle , \quad (14)$$

rather than to a single ONV as it would be the case for an orthonormal orbital basis. For the sake of completeness, we provide the proof for Eq. (14) in the Appendix which exploits the anticommutator relation in Eq. (10).

In the last decades, considerable efforts were made to make nonorthogonal approaches such as valence-bond theory^{52,61–65} and nonorthogonal CI^{51,66,67} efficient. The latter suffer from an increasing computational complexity compared to a standard orthonormal formalism^{68–76} because of the nonorthogonal molecular orbital (MO) basis. In the framework of second quantization, the additional complexity can be attributed to the non-vanishing anticommutator in Eq. (10). For example, evaluating efficiently a matrix element of the type $\langle \Psi | \mathcal{O} | \Phi \rangle$ in a nonorthogonal approach, where \mathcal{O} could be an arbitrary one-electron (two-electron) operator and $|\Psi\rangle$ and $|\Phi\rangle$ are many-particle wave functions optimized for two different sets of MOs, respectively, requires a generalization^{68,69,72} of the Slater-Condon rules^{77,78}.

In order to arrive at a formalism for evaluating matrix elements that closely resembles an orthonormal approach, the anticommutator in Eq. (11) must vanish. To this end, it is useful to define a new orbital basis $\bar{\varphi} = \{\bar{\varphi}_p\}$ through the transformation^{50,58,79},

$$\bar{\varphi} = \varphi \mathbf{S}^{-1} , \quad (15)$$

where $\{\bar{\varphi}_p\}$ is referred to as the *dual* of the nonorthogonal basis $\{\varphi_p\}$ ^{58,79}. Moreover, $\{\bar{\varphi}_p\}$ and $\{\varphi_p\}$ are said to form a *biorthonormal* system⁵⁰ since we have

$$\langle \bar{\varphi}_p | \varphi_q \rangle = \delta_{pq} , \quad (16)$$

and further, if both bases span the same space, they are jointly called a biorthonormal orbital basis. The definition of the biorthonormal creation operators follows from Eq. (15) as

$$\bar{a}_{p\sigma}^\dagger = \sum_r a_{r\sigma}^\dagger S_{rp}^{-1} . \quad (17)$$

To illustrate the biorthonormality, we consider the anticommutator for a biorthonormal creation operator with an annihilation operator in the original basis,

$$\{\bar{a}_{p\sigma}^\dagger, a_{q\tau}\} = \sum_r \{a_{r\sigma}^\dagger S_{rp}^{-1}, a_{q\tau}\} = \sum_r S_{rp}^{-1} \underbrace{\{a_{r\sigma}^\dagger, a_{q\tau}\}}_{=S_{qr}\delta_{\sigma\tau}} = \delta_{pq} \delta_{\sigma\tau} , \quad (18)$$

which yields the standard anticommutation relation (cf. Eq. (11)).

III. MATRIX PRODUCT STATES AND MATRIX PRODUCT OPERATORS

A. Concepts

We briefly introduce the concepts of expressing a quantum state as an MPS and a (Hermitian) operator as an MPO. Our notation follows the presentation of Ref. 56.

Consider an arbitrary state $|\Psi\rangle$ in a Hilbert space spanned by L spatial orbitals which we express as a linear superposition of ONVs $|\mathbf{k}\rangle$ with the CI coefficients $c_{k_1\dots k_L}$ as expansion coefficients

$$|\Psi\rangle = \sum_{\mathbf{k}} c_{\mathbf{k}} |\mathbf{k}\rangle = \sum_{k_1, \dots, k_L} c_{k_1 \dots k_L} |k_1 \dots k_L\rangle , \quad (19)$$

where each local space is of dimension four corresponding to the basis states $k_l = |\uparrow\downarrow\rangle, |\uparrow\rangle, |\downarrow\rangle, |0\rangle$ of a spatial orbital. In an MPS representation of $|\Psi\rangle$, we encode the CI coefficients $c_{k_1\dots k_L}$ as a product of $m_{l-1} \times m_l$ -dimensional matrices $M^{k_l} = \{M_{a_{l-1}a_l}^{k_l}\}$

$$|\Psi\rangle = \sum_{k_1, \dots, k_L} \sum_{a_1, \dots, a_{L-1}} M_{1a_1}^{k_1} M_{a_1 a_2}^{k_2} \dots M_{a_{L-1} 1}^{k_L} |k_1 \dots k_L\rangle = \sum_{\mathbf{k}} M^{k_1} M^{k_2} \dots M^{k_L} |\mathbf{k}\rangle , \quad (20)$$

where the last equality follows from collapsing the summation over the a_l indices (sometimes referred to as *virtual indices* or *bonds*) as matrix-matrix multiplications. Since the final contraction of the matrices M^{k_l} must yield the scalar coefficient $c_{k_1\dots k_L}$, the first and the last matrices are in practice $1 \times m_1$ -dimensional row and $m_{L-1} \times 1$ -dimensional column vectors, respectively. Allowing for the introduction of some maximum dimension m for the matrices M^{k_l} , with m commonly referred to as *number of renormalized block states*³¹, is the central idea that facilitates a reduction of the exponentially scaling full CI *ansatz* in Eq. (19) to a polynomial-scaling MPS wave function *ansatz*. For further details on the actual variational search algorithm for ground- and excited states in an MPS framework, we refer the reader to

the review by Schollwöck³³ and, for its formulation in a quantum chemical program package, for instance to our recent works^{56,57}.

We may express an operator \widehat{W} in MPO form

$$\begin{aligned}\widehat{W} &= \sum_{k_1, \dots, k_L} \sum_{k'_1, \dots, k'_L} \sum_{b_1, \dots, b_{L-1}} W_{1b_1}^{k_1 k'_1} W_{b_1 b_2}^{k_2 k'_2} \dots W_{b_{L-1} 1}^{k_L k'_L} |k_1 \dots k_L\rangle \langle k'_1 \dots k'_L| \\ &= \sum_{\mathbf{k} \mathbf{k}'} W^{k_1 k'_1} W^{k_2 k'_2} \dots W^{k_L k'_L} |\mathbf{k}\rangle \langle \mathbf{k}'| \equiv \sum_{\mathbf{k} \mathbf{k}'} w_{\mathbf{k} \mathbf{k}'} |\mathbf{k}\rangle \langle \mathbf{k}'| ,\end{aligned}\quad (21)$$

with the incoming and outgoing physical states k_l and k'_l and the virtual indices b_{l-1} and b_l . In analogy to Eq. (20), we may recognize the summation over pairwise matching indices b_l as matrix-matrix multiplications which leads to the second line on the right-hand side of Eq. (21). For practical applications, we rearrange the summations in Eq. (21) and contract first over the local site indices $k_l k'_l$

$$\widehat{W}_{b_{l-1} b_l} = \sum_{k_l k'_l} W_{b_{l-1} b_l}^{k_l k'_l} |k_l\rangle \langle k'_l| ,\quad (22)$$

which then yields

$$\widehat{W} = \sum_{b_1, \dots, b_{L-1}} W_{1b_1}^1 \dots W_{b_{l-1} b_l}^l \dots W_{b_{L-1} 1}^L .\quad (23)$$

The local, operator-valued matrix representation introduced in Eq. (22) is a central element for an efficient MPO-based implementation of the quantum-chemical DMRG approach^{56,57} that offers the same polynomial scaling as a “traditional” (non-MPO) DMRG implementation.

B. MPO expectation values with nonorthogonal orbitals

The calculation of overlap matrix elements and expectation values for N -electron operators in an MPO framework based on an orthonormal basis common for the bra and ket states was outlined, for instance, in Refs. 33 and 56, respectively. Here, we illustrate the complexity that results when the bra and ket states are expressed in two different MO bases which are in general not orthonormal.

Following the notation by Malmqvist and Roos⁴⁸, orbital basis superscripts X and Y denote the original (orthonormal) MO bases $\{\varphi_p^X\}$ and $\{\varphi_p^Y\}$, respectively, whereas the superscripts A and B refer to different MO bases $\{\varphi_p^A\}$ and $\{\varphi_p^B\}$, respectively, which have

been manipulated in some way and are therefore in general not orthonormal. We assume that the MPS wave functions are optimized with the same active orbital spaces and a common atomic orbital basis set. The latter restrictions can, however, be lifted^{50,80}.

1. General considerations

Let $|\Psi\rangle$ and $|\Phi\rangle$ denote two MPS wave functions based on the definition in Eq. (20),

$$|\Psi\rangle = \sum_{\mathbf{k}^A} \sum_{a_1, \dots, a_{L-1}} M_{1a_1}^{k_1^A} M_{a_1 a_2}^{k_2^A} \cdots M_{a_{L-1} 1}^{k_L^A} |\mathbf{k}^A\rangle, \quad (24)$$

$$|\Phi\rangle = \sum_{\mathbf{k}^B} \sum_{a'_1, \dots, a'_{L-1}} N_{1a'_1}^{k_1^B} N_{a'_1 a'_2}^{k_2^B} \cdots N_{a'_{L-1} 1}^{k_L^B} |\mathbf{k}^B\rangle, \quad (25)$$

which are constructed from MO sets $\{\varphi_p^A\}$ and $\{\varphi_p^B\}$, respectively.

We start by considering the overlap $\langle\Phi|\Psi\rangle$ which can be written as^{33,56,59}

$$\begin{aligned} \langle\Phi|\Psi\rangle &= \sum_{\mathbf{k}^A \mathbf{k}^B} \sum_{\substack{a_1, \dots, a_{L-1} \\ a'_1, \dots, a'_{L-1}}} \left(N_{1a'_{L-1}}^{k_{L-1}^B \dagger} \cdots N_{a'_2 a'_1}^{k_2^B \dagger} N_{a'_1 1}^{k_1^B \dagger} \right) \left(M_{1a_1}^{k_1^A} M_{a_1 a_2}^{k_2^A} \cdots M_{a_{L-1} 1}^{k_L^A} \right) \langle\mathbf{k}^B | \mathbf{k}^A\rangle \\ &= \sum_{\mathbf{k}^A \mathbf{k}^B} \sum_{\substack{a_1, \dots, a_{L-1} \\ a'_1, \dots, a'_{L-1}}} \left(N_{1a'_{L-1}}^{k_{L-1}^B \dagger} \cdots N_{a'_2 a'_1}^{k_2^B \dagger} N_{a'_1 1}^{k_1^B \dagger} \right) \left(M_{1a_1}^{k_1^A} M_{a_1 a_2}^{k_2^A} \cdots M_{a_{L-1} 1}^{k_L^A} \right) \\ &\quad \times \delta_{N_{\mathbf{k}^B} N_{\mathbf{k}^A}} \det \mathbf{S}^{\mathbf{k}^B \mathbf{k}^A}, \end{aligned} \quad (26)$$

with $N_{\mathbf{k}^B}$ and $N_{\mathbf{k}^A}$ being the number of electrons comprised in the ONVs and $\det \mathbf{S}^{\mathbf{k}^B \mathbf{k}^A}$ the determinant of the overlap matrix $\mathbf{S}^{\mathbf{k}^B \mathbf{k}^A}$ of all overlap integrals between occupied orbitals of the bra and ket ONVs. Compared to the standard expression of the inner product of ONVs that are built from a common orthonormal basis $\{\tilde{\varphi}\}$, implying for example $\{\varphi_p^A\} \equiv \{\varphi_p^B\}$,⁵⁹

$$\langle\mathbf{k}^B | \mathbf{k}^A\rangle = \prod_{p=1}^L \delta_{k_p^B k_p^A}, \quad (27)$$

the inner product in Eq. (26) leads to a rather complex expression with a large number of non-zero terms. The reason for the latter is that in the general case of nonorthogonal orbitals the action of an annihilator on a given ONV, as illustrated in Eq. (14), creates a sum of ONVs rather than a single ONV.

Turning next to transition matrix elements $\langle\Phi|\hat{\mathcal{O}}|\Psi\rangle$ of an N -electron operator $\hat{\mathcal{O}}$ given

in MPO form (cf. Eq (21)), the expression in the case of nonorthogonal orbitals reads

$$\begin{aligned}
\langle \Phi | \hat{\mathcal{O}} | \Psi \rangle &= \sum_{\mathbf{k}^A \mathbf{k}^B} \sum_{\substack{a_1, \dots, a_{L-1} \\ a'_1, \dots, a'_{L-1}}} \left(N_{1a'_{L-1}}^{k_L^B \dagger} \dots N_{a'_2 a'_1}^{k_2^B \dagger} N_{a'_1 1}^{k_1^B \dagger} \right) \\
&\times \langle \mathbf{k}^B | \left[\sum_{\mathbf{k}^{B'} \mathbf{k}^{B''}} \sum_{\mathbf{k}^{A'} \mathbf{k}^{A''}} \sum_{b_1 \dots b_{L-1}} \left(O_{1b_1}^{k_1^{B'} k_1^{A'}} O_{b_1 b_2}^{k_2^{B'} k_2^{A'}} \dots O_{b_{L-1} 1}^{k_L^{B'} k_L^{A'}} \right) | \mathbf{k}^{B'} \rangle \langle \mathbf{k}^{B''} | \mathbf{k}^{A''} \rangle \langle \mathbf{k}^{A'} | \right. \\
&\times \left. \left(M_{1a_1}^{k_1^A} M_{a_1 a_2}^{k_2^A} \dots M_{a_{L-1} 1}^{k_L^A} \right) | \mathbf{k}^A \rangle \right] . \tag{28}
\end{aligned}$$

Note that, similarly to Eq. (26), the inner product $\langle \mathbf{k}^{B''} | \mathbf{k}^{A''} \rangle$ of the ONVs will not simply reduce to a product of delta functions since the incoming and outgoing basis states of the operator are nonorthogonal. Moreover, the fermionic anticommutation which is encoded explicitly in the matrix representation of the creation and annihilation operators (see, in particular, Section IV in Ref. 56 for a detailed discussion) by using their Wigner-Jordan-transformed form⁸¹ will introduce additional overlap terms as becomes clear from the anticommutation rules in Eqs. (9) and (10).

If, however, we assume that $|\Psi\rangle$ and $|\Phi\rangle$ are expressed in a common, orthonormal basis

the wave function expansion parameters need to be transformed as well. Moreover, as already pointed out by Malmqvist and Roos⁴⁸, the objective is to find efficient wave function transformations from the original basis $\{\varphi_p^X\}$ ($\{\varphi_p^Y\}$) to the biorthogonal basis $\{\varphi_p^A\}$ ($\{\varphi_p^B\}$) *while explicitly avoiding* any additional wave function optimization. Such an algorithm was proposed by Malmqvist for CI-type wave functions⁴⁹. Following up on Malmqvist's original idea, we outline in the following how such a transformation can be achieved for MPS-type wave function expansions by a sequence of single-orbital replacements. Similarly to CI-type expansions, each step in the sequence is approximately twice as expensive to compute as the matrix-vector product

$$y = \widehat{\mathcal{T}}x . \quad (31)$$

for a one-electron-operator $\widehat{\mathcal{T}}$.

a. Orbital transformation Considering the biorthonormality condition (cf. Eq. (30)), Malmqvist⁴⁹ and Olsen *et al.*⁵⁰ showed that an LU-factorization of the inverse of the orbital overlap matrix $(\mathbf{S}^{XY})^{-1}$ defined according to Eq. (2) with the bra (ket) orbitals in $\{\varphi_p^X\}$ ($\{\varphi_p^Y\}$) yields

$$(\mathbf{S}^{XY})^{-1} = \mathbf{C}^{YB} (\mathbf{C}^{XA})^\dagger , \quad (32)$$

where \mathbf{C}^{XA} and \mathbf{C}^{YB} are the desired orbital transformation matrices. They allow us to express the biorthonormal bases $\{\varphi_p^A\}$ and $\{\varphi_p^B\}$ in terms of the original orbital bases $\{\varphi_p^X\}$ and $\{\varphi_p^Y\}$, respectively,^{49,50}

$$\varphi^A = \varphi^X \mathbf{C}^{XA} , \quad (33)$$

$$\varphi^B = \varphi^Y \mathbf{C}^{YB} . \quad (34)$$

Expressing the orbital transformation in Eq. (33) as a sequence of single orbital transformations the substitution of orbital φ_1^X reads^{49,50}

$$\varphi_1^X = \varphi_1^A t_{11} + \varphi_2^X t_{21} + \varphi_3^X t_{31} + \dots , \quad (35)$$

and for orbital φ_2^X

$$\varphi_2^X = \varphi_1^A t_{12} + \varphi_2^A t_{22} + \varphi_3^X t_{32} + \dots , \quad (36)$$

and so forth. Collecting the unknown parameters t_{mn} in a matrix \mathbf{t} and splitting it into upper (U) and lower (L) triangular parts \mathbf{t}_U and \mathbf{t}_L , respectively, the general sequence of transformations is given by^{49,50}

$$\varphi^X = \varphi^A \mathbf{t}_U + \varphi^X \mathbf{t}_L . \quad (37)$$

From the last equation, it follows that \mathbf{C}^{XA} can be written as^{49,50}

$$\mathbf{C}^{\text{XA}} = (\mathbf{1} - \mathbf{t}_L) \mathbf{t}_U^{-1} , \quad (38)$$

or, alternatively, in terms of an LU-factorization^{49,50} as

$$\mathbf{C}^{\text{XA}} = \mathbf{L}\mathbf{U} , \quad (39)$$

with \mathbf{L} being a lower triangular matrix with unit diagonal elements and \mathbf{U} an upper triangular matrix. Combining Eqs. (38) and (39) we can determine the upper and lower triangular parts of \mathbf{t}

$$\mathbf{t}_U = \mathbf{U}^{-1} \quad \text{and} \quad \mathbf{t}_L = \mathbf{1} - \mathbf{L} \quad (40)$$

The same considerations hold for \mathbf{C}^{YB} and its factorization into upper and lower triangular matrices.

b. MPS wave function transformation With the elements of the matrix \mathbf{t} at hand (*vide supra*), the wave function expansion parameters can be transformed by a sequence of single-orbital transformations^{49,50}. A detailed account of this transformation approach can be found for CI-type wave functions in Refs. 49 and 50. Following closely their *ansatz*, we outline below the essential steps required to transform an MPS-type wave function representation from an expansion in the original basis $\{\varphi_p^{\text{X}}\}$ to an expansion in a biorthonormal basis $\{\varphi_p^{\text{A}}\}$. As discussed in Subsection III B, the latter will allow us to calculate N -particle transition density matrices in a framework of standard second-quantization algebra.

We start by transforming the wave function $|\Psi\rangle$

$$|\Psi\rangle = \sum_{\mathbf{k}^{\text{X}}} M^{k_1^{\text{X}}} M^{k_2^{\text{X}}} \dots M^{k_L^{\text{X}}} |\mathbf{k}^{\text{X}}\rangle , \quad (41)$$

where we have introduced above an additional superscript X to emphasize that the MPS tensors of $|\Psi\rangle$ refer to the original orbital basis $\{\varphi^{\text{X}}\}$. With the parameters \mathbf{t}_L and \mathbf{t}_U calculated from an LU-factorization of \mathbf{C}^{XA} according to Eq. (40), the MPS wave function transformation proceeds differently for inactive and active orbitals. No special action is required for the secondary (virtual) orbital space.

Transformation with respect to the *inactive* orbital space As shown in Ref. 49, this transformation step reduces for CAS-type wave functions to a simple scaling of $|\Psi\rangle$ by

a factor α ,

$$|\Psi\rangle \equiv \alpha \cdot |\Psi\rangle = \sum_{\mathbf{k}^X} \alpha \cdot \left(M^{k_1^X} M^{k_2^X} \dots M^{k_L^X} \right) |\mathbf{k}^X\rangle \quad (42)$$

with

$$\alpha = \prod_{i=1}^{n_I} (t_{ii})^2, \quad (43)$$

where the inactive orbital space comprises n_I orbitals.

Transformation with respect to the active orbital space Assuming an active orbital space comprising L active orbitals, we set the orbital counter to $j = 1$ and proceed as follows:

1. Scale the j -th MPS tensor $M^{k_j^X}$ of $|\Psi\rangle$ consisting of a set of matrices (one for each basis state occupation k_j^X) with respect to the occupation number of the j -th orbital,

$$M^{k_j^X} \equiv \begin{cases} t_{jj}^2 \cdot M^{k_{j,|\uparrow\downarrow}^X} & \text{for } k_j^X = |\uparrow\downarrow\rangle \\ t_{jj} \cdot M^{k_{j,|\uparrow}^X} & \text{for } k_j^X = |\uparrow\rangle \\ t_{jj} \cdot M^{k_{j,|\downarrow}^X} & \text{for } k_j^X = |\downarrow\rangle \\ M^{k_{j,|0}^X} & \text{for } k_j^X = |0\rangle \end{cases}, \quad (44)$$

and

$$M^{k_i^X} \equiv M^{k_i^X} \quad \forall i \neq j \wedge i = 1, \dots, L. \quad (45)$$

2. Construct a new MPO $\widehat{\mathcal{W}}$ for the one-electron operator $\widehat{\mathcal{T}}$,

$$\widehat{\mathcal{T}} = \sum_{m \neq j}^L \sum_{\sigma} \frac{t_{mj}}{t_{jj}} a_{m\sigma}^\dagger a_{j\sigma}, \quad (46)$$

where the coefficients t_{mj} are given by the matrix elements of \mathbf{t}_L and \mathbf{t}_U , respectively. Note that σ denotes here the eigenvalue of the spin eigenfunction.

3. Carry out a sequence of MPO–MPS operations³³, starting with the *exact* product

(analogous to Section 5.1, page 140*f* of Ref. 33)

$$\begin{aligned}
|\Psi^{(1)}\rangle &= \widehat{\mathcal{W}}|\Psi\rangle \\
&= \sum_{\mathbf{k}^X \mathbf{k}^{X'}} \left(W^{k_1^X k_1^{X'}} W^{k_2^X k_2^{X'}} \dots W^{k_L^X k_L^{X'}} \right) \left(M^{k_1^{X'}} M^{k_2^{X'}} \dots M^{k_L^{X'}} \right) |\mathbf{k}^X\rangle \\
&= \sum_{\mathbf{k}^X \mathbf{k}^{X'}} \sum_{\mathbf{ab}} \left(W_{1b_1}^{k_1^X k_1^{X'}} W_{b_1 b_2}^{k_2^X k_2^{X'}} \dots W_{b_{L-1} 1}^{k_L^X k_L^{X'}} \right) \left(M_{1a_1}^{k_1^{X'}} M_{a_1 a_2}^{k_2^{X'}} \dots M_{a_{L-1} 1}^{k_L^{X'}} \right) |\mathbf{k}^X\rangle \\
&= \sum_{\mathbf{k}^X \mathbf{k}^{X'}} \sum_{\mathbf{ab}} \left(W_{1b_1}^{k_1^X k_1^{X'}} M_{1a_1}^{k_1^{X'}} \right) \left(W_{b_1 b_2}^{k_2^X k_2^{X'}} M_{a_1 a_2}^{k_2^{X'}} \right) \dots \left(W_{b_{L-1} 1}^{k_L^X k_L^{X'}} M_{a_{L-1} 1}^{k_L^{X'}} \right) |\mathbf{k}^X\rangle \\
&= \sum_{\mathbf{k}^X} \sum_{\mathbf{ab}} N_{(11)(b_1 a_1)}^{k_1^X} N_{(b_1 a_1)(b_2 a_2)}^{k_2^X} \dots N_{(b_{L-1} a_{L-1})(11)}^{k_L^X} |\mathbf{k}^X\rangle \\
&= \sum_{\mathbf{k}^X} N^{k_1^X} N^{k_2^X} \dots N^{k_L^X} |\mathbf{k}^X\rangle , \tag{47}
\end{aligned}$$

where the compact notation

$$N_{(b_{i-1} a_{i-1})(b_i a_i)}^{k_i^X} = \sum_{k_i^{X'}} W_{b_{i-1} b_i}^{k_i^X k_i^{X'}} M_{a_{i-1} a_i}^{k_i^{X'}} , \tag{48}$$

has been introduced in the second to last step on the right-hand side of Eq. (47).

4. Compress $|\Psi^{(1)}\rangle$ by means of a singular-value decomposition (SVD) with a truncation threshold ϵ of (at most) $\epsilon = 10^{-8}$. This is followed by

$$\begin{aligned}
|\Psi^{(2)}\rangle &= \widehat{\mathcal{W}}|\Psi^{(1)}\rangle \\
&= \sum_{\mathbf{k}^X \mathbf{k}^{X'}} \left(W^{k_1^X k_1^{X'}} W^{k_2^X k_2^{X'}} \dots W^{k_L^X k_L^{X'}} \right) \left(N^{k_1^X} N^{k_2^X} \dots N^{k_L^X} \right) |\mathbf{k}^X\rangle \\
&= \sum_{\mathbf{k}^X} \sum_{\mathbf{ab}} O_{(11)(b_1 a_1)}^{k_1^X} O_{(b_1 a_1)(b_2 a_2)}^{k_2^X} \dots O_{(b_{L-1} a_{L-1})(11)}^{k_L^X} |\mathbf{k}^X\rangle \\
&= \sum_{\mathbf{k}^X} O^{k_1^X} O^{k_2^X} \dots O^{k_L^X} |\mathbf{k}^X\rangle , \tag{49}
\end{aligned}$$

in complete analogy to Eq. (47).

5. Set $|\Psi\rangle \equiv |\Psi\rangle + |\Psi^{(1)}\rangle + \frac{1}{2} |\Psi^{(2)}\rangle$ and perform an SVD compression of $|\Psi\rangle$.
6. Increase the orbital counter j by one. If $j \leq L$ repeat steps (1)-(5), otherwise exit the transformation algorithm. Note that the final MPS tensors of $|\Psi\rangle$ now refer to an expansion in the biorthonormal basis $\{\bar{\varphi}^A\}$, for example,

$$M_i^{k_i^A} \equiv M_i^{k_i^X} \quad \forall i = 1, \dots, L , \tag{50}$$

such that we can express $|\Psi\rangle$ as

$$|\Psi\rangle = \sum_{\mathbf{k}^A} M^{k_1^A} M^{k_2^A} \dots M^{k_L^A} |\mathbf{k}^A\rangle \quad (51)$$

Having found a representation of $|\Psi\rangle$ in the biorthonormal basis $\{\bar{\varphi}_p^A\}$, we repeat the transformation steps above for the inactive and active orbital spaces of the MPS wave function $|\Phi\rangle$ with \mathbf{t}_L and \mathbf{t}_U calculated from an LU-factorization of \mathbf{C}^{YB} .

IV. THE STATE-INTERACTION APPROACH FOR MPS WAVE FUNCTIONS

With the overlap and transition matrix elements at hand, calculated from spin-free MPS wave functions (i.e., SU(2) invariant MPS wave functions $|\Psi(S)\rangle$ with a well-defined total spin quantum number S as, for instance implemented in the QCMAQUIS program⁵⁷) in a biorthonormal basis, we are now able not only to calculate Hamiltonian but also matrix elements for arbitrary one- and two-particle property operators such as transition dipole moments (from which we can calculate oscillator strengths), angular momentum eigenvalues and magnetic transition dipoles, or electric field gradients. Based on the discussion in the previous section, Fig. 1 illustrates the typical workflow of our MPS-SI approach where the MPSs are obtained from different DMRG-SCF optimizations. We implemented this scheme in a development version of the MOLCAS 8.0⁸² software which, to a large extent, exploits the existing framework of the CASSI/RASSI implementation for CI-type wave functions by Malmqvist and co-workers^{48,80}. Further details on the SI approach common to both CI-type and MPS wave functions can be found in Refs. 48 and 80 and we here provide only a brief summary of the most important steps as outlined in Fig. 1.

Considering only the lower triangular matrix of dimension $N(N + 1)$ originating from N converged spin-free (non- or scalar-relativistic) MPS wave functions of arbitrary spatial symmetry and total spin S , we first test whether the i -th MPS shares the same MO basis as the j -th state. If the outcome of the test is negative, both MPSs are transformed to the biorthonormal basis according to Section IIIB 2 b, before proceeding with the calculation of the wave function overlap and transition density matrix elements. The latter are then combined with the corresponding AO-integrals to evaluate property and Hamiltonian matrix

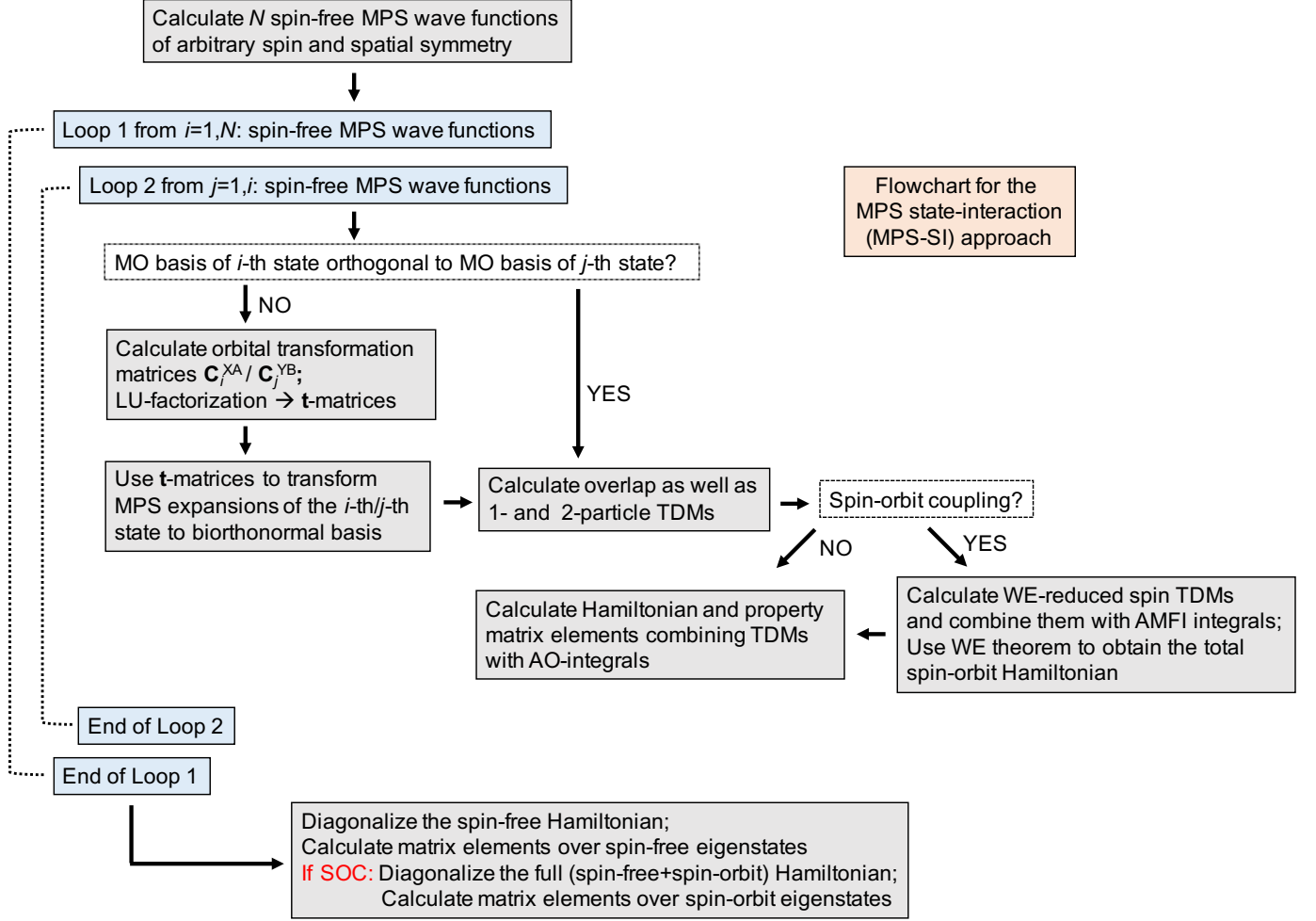


FIG. 1. The flowchart illustrates the MPS wave function state-interaction (MPS-SI) approach targeting property matrix elements of spin-free and spin-orbit coupled wave functions.

elements. In the last step we diagonalize the Hamiltonian matrix and calculate property matrix elements over the resulting N spin-free eigenstates.

Moreover, the calculation of magnetic properties such as g-tensors and hyperfine coupling tensors as well as the prediction of intersystem crossing rates requires access to SO coupled wave functions. To this end, we diagonalize the full Hamiltonian

$$\hat{\mathcal{H}} = \hat{\mathcal{H}}^{\text{el,sf}} + \hat{\mathcal{H}}^{\text{SO}}, \quad (52)$$

represented in the basis of the multiplet of states $|\Psi(S, M)\rangle$ that can be obtained from a spin-free calculation of $|\Psi(S)\rangle$. Here, the state label (S, M) indicates the pair of total spin S and spin magnetic quantum number M the latter which can take values in the range from $-S$ to S with unit increments. In our current approach, $\hat{\mathcal{H}}^{\text{el,sf}}$ is typically a scalar-relativistic,

spin-free electronic Hamiltonian, for example the Douglas-Kroll Hess Hamiltonian^{83–85} or the exact two-component Hamiltonian (X2C)^{86–89} with the energy expectation value E_A for the eigenfunction $|\Psi^A(S, M)\rangle$ of state A. For $\hat{\mathcal{H}}^{\text{SO}}$ we consider an effective one-electron mean-field SO Hamiltonian⁹⁰ in which the two-electron terms essentially serve as screening corrections of the (dominating) one-electron terms. Without significant loss of accuracy^{18,91} we apply an atomic-mean field approximation of the SO integrals as implemented in the AMFI program of B. Schimmelpfennig⁹² where all multicenter integrals are neglected. In the AMFI representation the effective one-electron mean-field SO Hamiltonian reads⁸⁰

$$\hat{\mathcal{H}}^{\text{SO}} = \sum_{pq} \left(V_{pq}^x \hat{\mathbf{T}}_{pq}^x + V_{pq}^y \hat{\mathbf{T}}_{pq}^y + V_{pq}^z \hat{\mathbf{T}}_{pq}^z \right), \quad (53)$$

where \mathbf{V}_{pq} are the AO spin-orbit interaction integrals and \mathbf{T}_{pq} the triplet operators in Cartesian representation. The latter are related to the more common triplet operators in spin-tensor form⁵⁹

$$\hat{\mathbf{T}}_{pq}^{1,1} = -a_{p\alpha}^\dagger a_{q\beta}, \quad (54)$$

$$\hat{\mathbf{T}}_{pq}^{1,0} = \frac{1}{\sqrt{2}} \left(a_{p\alpha}^\dagger a_{q\alpha} - a_{p\beta}^\dagger a_{q\beta} \right), \quad (55)$$

$$\hat{\mathbf{T}}_{pq}^{1,-1} = a_{p\beta}^\dagger a_{q\alpha}, \quad (56)$$

through a linear transformation⁵⁹,

$$\left(\hat{\mathbf{T}}_{pq}^x, \hat{\mathbf{T}}_{pq}^y, \hat{\mathbf{T}}_{pq}^z \right) = \left(\hat{\mathbf{T}}_{pq}^{1,1}, \hat{\mathbf{T}}_{pq}^{1,-1}, \hat{\mathbf{T}}_{pq}^{1,0} \right) \begin{pmatrix} -\frac{1}{2} & -\frac{1}{2i} & 0 \\ \frac{1}{2} & -\frac{1}{2i} & 0 \\ 0 & 0 & \frac{1}{\sqrt{2}} \end{pmatrix}. \quad (57)$$

Here, $\hat{\mathbf{T}}^{S,M}$ is a spin-tensor operator whose eigenfunctions are a tensor state with spin eigenvalues S and M . It is one of the $2S + 1$ spin-tensor operators comprising the spin-tensor operator $\hat{\mathbf{T}}^S$ of half-integer or integer rank S . To calculate the matrix representation of the SO operator given in Eq. (53) we need to evaluate matrix elements between state $|\Psi^A(S', M')\rangle$ and state $|\Psi^B(S'', M'')\rangle$ of the form $\langle \Psi^A(S', M') | \hat{\mathbf{T}}^{S,M} | \Psi^B(S'', M'') \rangle$. These can be calculated very efficiently by employing the Wigner-Eckart (WE) theorem^{5,93} which states that the $(2S' + 1) \times (2S + 1) \times (2S'' + 1)$ matrix elements above can be obtained as a product from a single (WE-reduced) matrix element $\langle \Psi^A(S') | | \hat{\mathbf{T}}^S | | \Psi^B(S'') \rangle$ and a Wigner

3j-symbol (calculated from Clebsch-Gordon coefficients),

$$\begin{aligned} \left\langle \Psi^A(S', M') \left| \hat{\mathbf{T}}^{S, M} \right| \Psi^B(S'', M'') \right\rangle &= (-1)^{S''+M'-S} \\ &\times \begin{pmatrix} S'' & S & S' \\ M'' & M & M' \end{pmatrix} \left\langle \Psi^A(S') \left\| \hat{\mathbf{T}}^S \right\| \Psi^B(S'') \right\rangle . \end{aligned} \quad (58)$$

Taking advantage of the WE theorem, we calculate WE-reduced one-particle (spin) transition density matrices⁸⁰

$$\Gamma_{pq}^{\text{WE}} = \left\langle \Psi^A(S') \left\| \hat{\mathbf{T}}_{pq}^S \right\| \Psi^B(S'') \right\rangle , \quad (59)$$

which can now be employed to calculate a WE-reduced matrix element⁸⁰

$$\mathbf{V}^{\text{AB}} = \sum_{pq} \Gamma_{pq}^{\text{WE}} \mathbf{V}_{pq} . \quad (60)$$

Since the matrix elements over spin states will only be non-zero if $|S'' - S'|$ is an integer ≤ 1 , while also $|M'' - M'|$ is an integer ≤ 1 , we are left with a total of nine non-zero SO Hamiltonian matrix elements, for example,

$$\left\langle \Psi^A(SM) \left| \hat{H}^{\text{SO}} \right| \Psi^B(S+1M\pm 1) \right\rangle = -\frac{\sqrt{(S\pm M+1)(S\pm M+2)}}{2} (\pm V^{\text{AB},x} + iV^{\text{AB},y}) \quad (61)$$

and

$$\left\langle \Psi^A(SM) \left| \hat{H}^{\text{SO}} \right| \Psi^B(SM) \right\rangle = MV^{\text{AB},z} , \quad (62)$$

where the remaining six cases can be found in Ref. 80.

With the matrix elements of the SO operator at hand, we next diagonalize the total Hamiltonian matrix \mathbf{H} of the Hamiltonian \mathcal{H} given in Eq. (52) with the matrix elements given by

$$\left\langle \Psi^A(S'M') \left| \hat{\mathcal{H}} \right| \Psi^B(S''M'') \right\rangle = S_{\text{AB}} \delta_{S'S''} \delta_{M'M''} E_A + \left\langle \Psi^A(S'M') \left| \hat{H}^{\text{SO}} \right| \Psi^B(S''M'') \right\rangle , \quad (63)$$

where S_{AB} is the overlap between states A and B. Note that it is also possible, prior to the diagonalization of \mathbf{H} , to correct the state energies for dynamic electron correlation contributions from, e.g., a DMRG-CASPT2^{94–96} or DMRG-NEVPT2^{97–101} calculation by shifting the diagonal elements of the total Hamiltonian by⁸⁰

$$\Delta H_{\text{AB}} = 0.5 (\Delta E_A + \Delta E_B) S_{\text{AB}} , \quad (64)$$

where ΔE_A is the dynamical electron correlation contribution shift for state A.

Diagonalization of \mathbf{H} yields a set of SO coupled eigenstates which are linear combinations of all MPS wave functions with different spin and magnetic quantum numbers and the corresponding eigenvalues. In the final step (lower box in Fig. 1), we can now calculate the desired property matrix elements such as g-tensor matrix elements (see for example Ref. 9 for further details) in the basis of the SO eigenstates.

V. NUMERICAL EXAMPLES

A. Closedness of MPS wave function expansion

The transformation algorithm outlined in Section IIIB2b is based on Malmqvist’s approach⁴⁹ which can only be applied to wave function expansions that are closed under de-excitation^{53–55}. The latter implies that in each sequence of the wave function transformation no states outside of the original wave function expansion are generated. This prerequisite is fulfilled by full CI wave functions and was also shown to be the case for restricted active space wave functions⁵³. Here, we probe the closedness and (approximate) orbital rotation invariance of our MPS wave function transformation by systematically increasing the numerical accuracy of the MPS with a varying number of renormalized block states m for a given active orbital space. As an example, we choose to study the zero-field splitting (ZFS) of the spin-free ground state ${}^3\Sigma_g^-$ of the tellurium dimer Te_2 for which CASSCF-SO reference data are available¹⁰² for both the ZFS and the SO matrix element V between the spin-free ${}^3\Sigma_g^-$ and ${}^1\Sigma_g^+$ states.

In accordance with the reference work of Rota *et al.*¹⁰², we employ an all-electron ANO-RCC basis set of TZP quality^{103,104} for Te along with the 2nd-order Douglas-Kroll-Hess (DKH2) scalar-relativistic Hamiltonian¹⁰⁵. The internuclear Te-Te distance of 2.557 Å is taken from experiment¹⁰⁶. In the chalcogenide dimers, the low-lying electronic spectrum originates from the valence $(\pi^*)^2$ configuration which gives rise to the $X\ 0_g^+$ electronic ground and $X_2\ 1_g, a\ 2_g$ and $b\ 0_g^+$ excited states. We consider a CAS(8,6) with 8 electrons allowed to freely occupy the six spatial orbitals (σ, σ^*, π and π^*) resulting from combinations of the atomic Te $5p$ valence orbitals. For this active orbital space, we carried out individual state-averaged spin-free DMRG-SCF calculations for five triplet and six singlet states which are subsequently allowed to mix through SO interaction in our MPS-SI *ansatz*. The latter

requires a transformation to a biorthonormal MO basis and a corresponding rotation of the MPS wave functions to this basis. We therefore expect that any significant violation of the closedness and/or orbital rotation invariance of the MPS *ansatz* for finite values of m would lead to considerable differences in the calculated spectrum and/or the SO matrix element V compared to the reference CASSCF data.

All results are compiled in Table I. We first note that for the small CAS(8,6) space all our DMRG-SCF-SO data for the ZFS and the SO matrix element V , irrespective of the number of renormalized block states m ranging from $m = 64$ to $m = 2048$, is in excellent agreement with the reference CASSCF-SO data (third-to-last row in Table I) obtained in this work. This result may not be surprising at first glance because of the size of the considered CAS but it nevertheless indicates that the closedness assumption holds for full CI-type wave functions represented by MPS expansions with finite m values. Moreover, orbital rotation invariance which is in principle only fulfilled exactly for MPS wave function expansions with $m \rightarrow \infty$ appear not to have an impact on our MPS transformation approach to the biorthonormal basis.

Compared to the CASSCF-SO data by Rota *et al.*, our DMRG-SCF-SO/CASSCF-SO data deviate by several hundred wave numbers for the excitation energies of the spin-free and SO coupled excited states as well as by 25 cm^{-1} for the SO matrix element V . This is partly due to the fact that we took into account only the lowest five (six) triplet (singlet) states in the wave function optimization. Considering all spin-free states up to 70000 cm^{-1} (second-to-last row in Table I) partly reduces the observed deviations, in particular for V . In summary, we emphasize that our CASSCF-SO and DMRG-SCF-SO data are consistent.

B. Magnetic resonance properties of sample f^1 and f^2 actinide complexes

To illustrate the capabilities of our MPS-SI approach, we calculate g-factors of prototypical f^1 - and f^2 -type actinide complexes, namely NpO_2^{2+} and PuO_2^{2+} , and compare to CASSCF/CASPT2 data from Gendron *et al.*¹⁰⁷. To facilitate a comparison, we follow the same computational protocol as outlined in Ref. 107 which we briefly summarize here. We employed all-electron ANO-RCC basis sets of TZP quality^{103,104} along with the scalar-relativistic DKH2 Hamiltonian¹⁰⁵ and a Cholesky-decomposition (CD) of the two-electron repulsion integrals as implemented in MOLCAS⁸² (keyword `Cholesky` in the integral mod-

TABLE I. Relative first excited state energies of Te_2 as obtained from spin-free (SF) and spin-orbit coupled (SOC) DMRG-SCF calculations with a varying number of renormalized block states m . V denotes the spin-orbit coupling matrix element between the ${}^3\Sigma_g^-$ and ${}^1\Sigma_g^+$ states. All values are given in cm^{-1} .

method	CAS	m	SF		SOC			V
			${}^1\Delta_g$	${}^1\Sigma_g^+$	X_21_g	$a2_g$	$b\ 0_g^+$	
DMRG-SCF-SO	(8,6)	64	3712	6588	1759	5471	10107	3832
DMRG-SCF-SO	(8,6)	128	3711	6587	1759	5471	10106	3832
DMRG-SCF-SO	(8,6)	256	3711	6587	1759	5470	10105	3832
DMRG-SCF-SO	(8,6)	512	3711	6586	1759	5470	10105	3832
DMRG-SCF-SO	(8,6)	1024	3711	6587	1759	5470	10105	3832
DMRG-SCF-SO	(8,6)	2048	3711	6586	1759	5470	10105	3832
CASSCF-SO ^a	(8,6)	-	3711	6586	1759	5470	10105	3832
CASSCF-SO ^b	(8,6)	-	3507	6298	1657	4917	9317	3808
CASSCF-SO ^c	(8,6)	-	2716	6009	1700	4180	9153	3807

^a This work.

^b This work. All spin-free states up to $70,000\ \text{cm}^{-1}$ were considered.

^c Ref. 102; CAS(8,6)SCF-SO/TZP data.

ule SEWARD). Dynamical electron correlation is included through CD-DMRG-NEVPT2 (second order n -electron valence perturbation theory) calculations^{43,101} with a state-averaged DMRG-SCF reference wave function. Active orbital spaces for the latter comprise 7 (8) electrons in 10 orbitals for NpO_2^{2+} (PuO_2^{2+}) denoted in the following as CAS(7,10) (CAS(8,10)). For NpO_2^{2+} , we simultaneously optimized six doublet states while for PuO_2^{2+} we carried out individual state-averaged DMRG-SCF calculations for 20 triplet and 20 singlet states, respectively. In all DMRG-SCF calculations, the number renormalized block states m was set to 1024 which is sufficient to yield results of CASSCF quality for the active orbital spaces considered. In accordance with Gendron *et al.*¹⁰⁷, C_1 point group symmetry was assumed in calculations.

As outlined in Section IV, our MPS-SI approach is integrated in the CASSI/RASSI framework^{48,80} of MOLCAS which allowed us to calculate the SO operator matrix elements

from the contraction of WE-reduced spin transition density matrices with atomic mean-field integrals^{90,92} while EPR g-factors were calculated based on the approach of Bolvin⁹.

In the case of Np(VI)O_2^{2+} we carried out additional four-component EPR calculations using a multi-reference CI (MRCI) approach¹¹ based on the Dirac-Coulomb Hamiltonian and all-electron uncontracted cc-pVTZ¹⁰⁸ and dyall.v3z¹⁰⁹ basis sets for oxygen and neptunium, respectively. MP2 natural spinors obtained from correlating the Np 5s5p5d6s6p and O 2s2p electrons while keeping the remaining core electrons of Np and O frozen constitute the orbital basis for the MRCI expansion. In the MP2 calculation, a virtual spinor threshold was set to 20 hartree such that the virtual correlation space comprised all recommended core-valence and valence-correlation functions. The MRCI active space includes all occupied spinors with occupation numbers less than 1.98 as well as all virtual spinors with occupation numbers up to about 0.001. The active space was further split in three subspaces with a maximum allowed excitation level of singles and singles-doubles from the first space containing all spinors with occupation larger than 1.80 into a model space comprising the four partially occupied nonbonding Np 5f spinors of Np(VI)O_2^{2+} ¹⁰⁷. From the combined two lower spaces a maximum of singles-doubles-triples excitations are allowed into the third space comprising in total 90 spinors.

Table II summarizes our property calculations for NpO_2^{2+} and PuO_2^{2+} . Starting with NpO_2^{2+} , we note that our DMRG/NEVPT2-SO results are in close agreement with the corresponding CASSCF/CASPT2-SO data from Gendron *et al.*¹⁰⁷ both for the g-factors, g_{\parallel} and g_{\perp} , respectively, and the vertical excitation energy ΔE from the ${}^2\Phi_{5/2u}$ ground to the ${}^2\Delta_{3/2u}$ first excited state. The DMRG/NEVPT2-SO $g_{\parallel} = 4.235$ value for NpO_2^{2+} compares further well with our reference four-component MRCI $g_{\parallel} = 4.283$ value which indicates that the considered number of spin-free states is sufficient to achieve convergence of the SO coupling contributions. Moreover, we find that the ground- and excited state compositions of the SO coupled ${}^2\Phi_{5/2u}$ and ${}^2\Delta_{3/2u}$ states in terms of their ϕ , δ and π character are well reproduced in our DMRG/NEVPT2-SO calculation in comparison to the CASSCF/CASPT2-SO reference data, in particular the sizable admixture of 12% δ character in the SO coupled ${}^2\Phi_{5/2u}$ ground state which originates from a strong coupling of the spin-free ${}^2\Phi_u$ and ${}^2\Delta_u$ states¹⁰⁷.

Turning next to PuO_2^{2+} , we find an excellent agreement of our DMRG-SCF-SO results for the electronic $\Omega = 4_g$ ground and the lowest-lying excited states with the corresponding CASSCF-SO reference data by Gendron *et al.*¹⁰⁷. We are not only able to correctly reproduce

the ground-state g-factors of $g_{\parallel} = 6.076$ and $g_{\perp} = 0.000$ but also find matching vertical excitation energies ΔE with deviations of at most 5 cm^{-1} for the first three excited states. Similar to NpO_2^{2+} , the lowest spin-free states of the plutonyl ion originate from occupations of the non-bonding δ and ϕ orbitals with different combinations (parallel or antiparallel) of spin (M_S) and angular momentum (M_L) projections. In accordance with Hund’s rules, the spin-free ground state is a 3H_g ($\delta^1\phi^1$ occupation) triplet state with parallel angular momentum projections ($M_L = \pm 2 \pm 3 = \pm 5$) and antiparallel spin projection $M_S = \mp 1$. Further combinations of M_S and M_L within the $\delta^1\phi^1$ occupation manifold lead to ${}^3\Sigma_g^-$ and ${}^3\Pi_g$ states which we find at 3875 cm^{-1} and 6563 cm^{-1} above the 3H_g ground state, respectively. Moreover, according to our DMRG-SCF calculations the first spin-singlet state ${}^1\Sigma_g^+$ is located at 10384 cm^{-1} above the electronic ground state.

At the SO level, the 3H_g term splits into its three components with $\Omega = 4_g, 5_g,$ and 6_g which are then allowed to mix with states of the same Ω . Although the $\Omega = 4_g$ ground state remains predominantly of 3H_g character (96%), it exhibits an admixture of the ${}^1\Gamma_g$ state (2%) which is energetically separated from the 3H_g state by about 15300 cm^{-1} in the spin-free framework. In addition, as can be seen from Table II, the first two SO-coupled excited states of $\Omega = 0_g^+$ and $\Omega = 1_g$ at $\Delta E = 4383 \text{ cm}^{-1}$ and 6985 cm^{-1} , respectively, originate from a strong admixture of different triplet and singlet states. Their state composition, as obtained from our DMRG-SCF-SO calculations, compares nicely with the CASSCF-SO data of Gendron *et al.*¹⁰⁷.

VI. CONCLUSIONS AND OUTLOOK

In this work, we presented a state-interaction (SI) approach for nonorthogonal matrix product state (MPS) wave functions dubbed as MPS-SI where the MPSs can be obtained from several different (state-specific) DMRG-SCF wave function optimizations. Our MPS-SI approach complements existing implementations for traditional CI-type wave functions while generalizing earlier SI approaches for DMRG wave functions to nonorthogonal wave functions as basis set for the MPS-SI approach.

Allowing for nonorthogonality of the input MPS wave functions adds a greater flexibility to the preceding orbital optimization step, which will be particularly beneficial for transition metal and lanthanide/actinide compounds, where state-specific optimizations allow

TABLE II. Relative energies ΔE [cm^{-1}], g-factors (absolute values), and state composition of the two lowest-energy electronic states of NpO_2^{2+} as well as the lowest electronic states of PuO_2^{2+} as obtained from DMRG-SCF-SO and DMRG/NEVPT2-SO calculations. The same active orbital space was employed as for the CASSCF-SO/CASPT2-SO data taken from the work of Gendron *et al.*¹⁰⁷. For details on the 4c-MRCI calculation, see text.

		NpO_2^{2+}			
		DMRG-SCF-SO	NEVPT2-SO	CASPT2-SO ^a	4c-MRCI
ground state	ΔE	0	0	0	0
$^2\Phi_{5/2u}$	g_{\parallel}	4.228	4.235	4.233	4.283
	g_{\perp}^b	0.002	0.002	0.002	0.000
	composition	89% ϕ , 11% δ	88% ϕ , 12% δ	88% ϕ , 12% δ	-
1st excited state	ΔE	3294	3086	3107	-
$^2\Delta_{3/2u}$	g_{\parallel}	2.025	2.035	2.037	-
	g_{\perp}^b	0.002	0.017	0.005	-
	composition	99% δ , 1% π	98% δ , 2% π	98% δ , 2% π	-
		PuO_2^{2+}			
		DMRG-SCF-SO	CASSCF-SO ^a		
ground state	ΔE	0	0		
4_g	g_{\parallel}	6.076	6.076		
	g_{\perp}	0.000	0.000		
	composition	96% 3H_g , 2% $^1\Gamma_g$	96% 3H_g		
1st excited state	ΔE	4383	4388		
0_g^+	composition	57% $^3\Sigma_g^-$, 27% $^3\Pi_g$, 14% $^1\Sigma_g^+$	57% $^3\Sigma_g^-$, 27% $^3\Pi_g$, 14% $^1\Sigma_g^+$		
2nd excited state	ΔE	6985	6985		
1_g	composition	36% $^3\Sigma_g^-$, 48% $^3\Pi_g$, 14% $^1\Pi_g$	35% $^3\Sigma_g^-$, 50% $^3\Pi_g$, 14% $^1\Pi_g$		
3rd excited state	ΔE	7150	7152		
5_g	composition	99% 3H_g	99% 3H_g		

^a Ref. 107; CAS(7,10)PT2-SO data for NpO_2^{2+} and CAS(8,10)SCF-SO data for PuO_2^{2+} .

^b A non-zero value for g_{\perp} indicates a minor symmetry-breaking in the optimized spin-free wave functions due to the neglect of point group symmetry.

us to explicitly consider different open-shell d - or f -orbital occupations. Moreover, our nonorthogonal MPS-SI approach no longer requires a state averaging of molecular states with different spin symmetry at the orbital optimization step if, for example, spin-orbit coupling elements between these states are to be calculated. In this work, we discussed the transformation of orbitals and MPS wave functions from a nonorthogonal to a biorthonormal basis by formulating a nonunitary orbital transformation algorithm for MPS wave functions. This opens up for an efficient calculation of overlap matrix elements between nonorthogonal MPS wave functions and matrix elements of the one- and two-particle reduced transition density matrix as well as of the spin-orbit operator. After diagonalization of the resulting spin-free and spin-orbit Hamiltonian matrices target properties are calculated in the basis of the corresponding *orthogonal and non-interacting* (spin-orbit coupled) eigenstates.

We demonstrated the applicability of the nonorthogonal MPS-SI approach for two example open-shell f^n actinide molecules, namely NpO_2^{2+} (f^1 complex) and PuO_2^{2+} (f^2 complex) for which we calculated ground- and excited-state properties including g-factors. Our spin-orbit DMRG-SCF/NEVPT2 g-factors for the two lowest doublet states of NpO_2^{2+} agree well with corresponding CASSCF/CASPT2 data reported in the literature. The ground-state g-factors are close to the values obtained from a four-component MRCI g-tensor calculation which includes spin-orbit coupling variationally from the outset. This indicates that the property values are (close to being) converged with respect to the number of spin-free states included in our MPS-SI approach. Subsequently, we carried out DMRG-SCF g-factor calculations for PuO_2^{2+} by allowing the lowest spin-free singlet and triplet states to interact through spin-orbit coupling. We found a similar agreement of our DMRG-SCF results to the CASSCF values as was the case for NpO_2^{2+} which illustrates that our nonorthogonal MPS-SI approach works equally well for cases where the interacting states do not share the same molecular orbital basis. Combined with our recently developed Cholesky-decomposition DMRG-NEVPT2 implementation, our MPS-SI approach will be valuable not only for the study of (magnetic) properties of transition metal and/or heavy-element complexes in different spin states but also for the full exploration of the photophysics and, more generally, excited-state (surface hopping) dynamics of chromophores and light-harvesting materials. The latter requires, besides the calculation of non-adiabatic coupling elements to locate and characterize conical intersections, the determination of intersystem crossing probabilities between electronic states of different spin multiplicity induced by spin-orbit coupling.

ACKNOWLEDGMENTS

This work was supported by the Schweizer Nationalfonds. SK is grateful to Prof. H. J. Aa. Jensen (SDU Odense) for providing him access to the four-component MRCI-EPR module. JA acknowledges support from the U.S. Department of Energy, Office of Basic Energy Sciences, Heavy Element Chemistry program, under grant de-sc0001136 (formerly DE-FG02-09ER16066).

APPENDIX

The action of an annihilation operator in a nonorthogonal basis

An annihilation operator in a nonorthogonal spin-orbital basis acting on an ONV is considered here. We follow closely the derivation that can be found in Ref. 59. Assume an ONV for L spin-orbitals as it was given in Eq. (12). Recalling that annihilation of the vacuum state is impossible,

$$a_{q\sigma} |\text{vac}\rangle = \sum_p S_{qp}^{1/2} \underbrace{\tilde{a}_{p\sigma}}_{=0 \ \forall p} |\text{vac}\rangle = 0, \quad (\text{A1})$$

we write the action of an annihilation operator on the ONV as (anti-)commutator of the annihilation operator and the product of even (odd) numbers of creation operators

$$\begin{aligned} a_{q\sigma} |\mathbf{k}\rangle &= \left(a_{q\sigma} \left(\prod_{p=1}^L (a_{p\sigma}^\dagger)^{k_{p\sigma}} \right) \mp \underbrace{\left(\prod_{p=1}^L (a_{p\sigma}^\dagger)^{k_{p\sigma}} \right) a_{q\sigma}}_{=0} \right) |\text{vac}\rangle \\ &= \begin{cases} \left[a_{q\sigma}, \prod_{p=1}^L (a_{p\sigma}^\dagger)^{k_{p\sigma}} \right] |\text{vac}\rangle & \text{for even } L \\ \left\{ a_{q\sigma}, \prod_{p=1}^L (a_{p\sigma}^\dagger)^{k_{p\sigma}} \right\} |\text{vac}\rangle & \text{for odd } L \end{cases}. \end{aligned} \quad (\text{A2})$$

The (anti-)commutator appearing in Eq. (A2) can be written in terms of linear combinations of a basic anticommutator of an annihilation and an creation operator exploiting the

corresponding operator identity

$$\left. \begin{array}{l} [\hat{\mathcal{A}}, \hat{\mathcal{B}}_1 \cdots \hat{\mathcal{B}}_L] \\ \{\hat{\mathcal{A}}, \hat{\mathcal{B}}_1 \cdots \hat{\mathcal{B}}_L\} \end{array} \right\} = \sum_{p=1}^L (-1)^{p-1} \hat{\mathcal{B}}_1 \cdots \{\hat{\mathcal{A}}, \hat{\mathcal{B}}_p\} \cdots \hat{\mathcal{B}}_L . \quad (\text{A3})$$

Inserting Eq. (A3) into the right-hand side of Eq. (A2) yields

$$a_{q\sigma} |\mathbf{k}\rangle = \sum_{p=1}^L k_{p\sigma} (-1)^{\left[\sum_{j=1}^{p-1} k_{j\sigma}\right]} \left(a_{1\sigma}^\dagger\right)^{k_{1\sigma}} \cdots \underbrace{\left\{a_{q\sigma}, \left(a_{p\sigma}^\dagger\right)^{k_{p\sigma}}\right\}}_{=S_{qp}\delta_{\sigma\sigma}} \cdots \left(a_{L\sigma}^\dagger\right)^{k_{L\sigma}} |\text{vac}\rangle . \quad (\text{A4})$$

Resolving the anticommutator by the identity in Eq. (10), as indicated in Eq. (A4), yields the final result

$$a_{q\sigma} |\mathbf{k}\rangle = \sum_{p=1}^L k_{p\sigma} (-1)^{\left[\sum_{j=1}^{p-1} k_{j\sigma}\right]} S_{qp} |k_1 k_2 \dots 0_p \dots k_L\rangle . \quad (\text{A5})$$

REFERENCES

- ¹M. Barbatti, WIREs Comput. Mol. Sci. **1**, 620 (2011).
- ²S. Mai, P. Marquetand, and L. González, Int. J. Quant. Chem. **115**, 1215 (2015).
- ³N. Suaud, M.-L. Bonnet, C. Boilleau, P. Labèguerie, and N. Guihéry, J. Am. Chem. Soc. **131**, 715 (2009).
- ⁴J. Chang, A. J. Fedro, and M. van Veenendaal, Phys. Rev. B **82**, 075124 (2010).
- ⁵C. M. Marian, WIREs Comp. Mol. Sci. **2**, 187 (2012).
- ⁶M. Kaupp, M. Bühl, and V. G. Malkin, eds., *Calculation of NMR and EPR Parameters: Theory and Applications* (Wiley-VCH, 2004).
- ⁷M. Gerloch and R. F. McMeeking, J. Chem. Soc., Dalton Trans. , 2443 (1975).
- ⁸H. Bolvin and J. Autschbach, in *Handbook of Relativistic Quantum Chemistry*, edited by W. Liu (Springer, Berlin, 2016).
- ⁹H. Bolvin, ChemPhysChem **7**, 1575 (2006).
- ¹⁰D. Ganyushin and F. Neese, J. Chem. Phys. **138**, 104113 (2013).
- ¹¹M. S. Vad, M. N. Pedersen, A. Nørager, and H. J. A. Jensen, J. Chem. Phys. **138**, 214106 (2013).
- ¹²K. Sharkas, B. Pritchard, and J. Autschbach, J. Chem. Theory Comput. **11**, 538 (2015).
- ¹³E. van Lenthe, P. E. S. Wormer, and A. van der Avoird, J. Chem. Phys. **107**, 2488 (1997).

- ¹⁴M. Repisky, S. Komorovsky, E. Malkin, O. L. Malkina, and V. G. Malkin, *Chem. Phys. Lett.* **488**, 94 (2010).
- ¹⁵P. Verma and J. Autschbach, *J. Chem. Theory Comp.* **9**, 1932 (2013).
- ¹⁶G. H. Lushington and F. Grein, *Int. J. Quant. Chem.* **60**, 1679 (1996).
- ¹⁷S. Brownridge, F. Grein, J. Tatchen, M. Kleinschmidt, and C. M. Marian, *J. Chem. Phys.* **118**, 9552 (2003).
- ¹⁸F. Neese, *J. Chem. Phys.* **122**, 034107 (2005).
- ¹⁹S. Vancoillie, P.-Å. Malmqvist, and K. Pierloot, *ChemPhysChem* **8**, 1803 (2007).
- ²⁰F. Neese, *Mol. Phys.* **105**, 2507 (2007).
- ²¹J. Tatchen, M. Kleinschmidt, and C. M. Marian, *J. Chem. Phys.* **130**, 154106 (2009).
- ²²M. Roemelt, *J. Chem. Phys.* **143**, 044112 (2015).
- ²³E. R. Sayfutyarova and G. K.-L. Chan, *J. Chem. Phys.* **144**, 234301 (2016).
- ²⁴P. G. Szalay, T. Müller, G. Gidofalvi, H. Lischka, and R. Shepard, *Chem. Rev.* **112**, 108 (2012).
- ²⁵D. Roca-Sanjuan, F. Aquilante, and R. Lindh, *WIREs Comp. Mol. Sci.* **2**, 585 (2012).
- ²⁶C. J. Stein, V. von Burg, and M. Reiher, *J. Chem. Theory Comput.* **12**, 3764 (2016).
- ²⁷J. Olsen, *Int. J. Quantum Chem.* **111**, 3267 (2011).
- ²⁸C. J. Stein and M. Reiher, *J. Chem. Theory Comput.* **12**, 1760 (2016).
- ²⁹F. Aquilante, J. Autschbach, R. K. Carlson, L. F. Chibotaru, M. G. Delcey, L. De Vico, I. Fdez. Galván, N. Ferré, L. M. Frutos, L. Gagliardi, M. Garavelli, A. Giussani, C. E. Hoyer, G. Li Manni, H. Lischka, D. Ma, P. A. Malmqvist, T. Müller, A. Nenov, M. Olivucci, T. B. Pedersen, D. Peng, F. Plasser, B. Pritchard, M. Reiher, I. Rivalta, I. Schapiro, J. Segarra-Martí, M. Stenrup, D. G. Truhlar, L. Ungur, A. Valentini, S. Vancoillie, V. Veryazov, V. P. Vysotskiy, O. Weingart, F. Zapata, and R. Lindh, *J. Comput. Chem.* **37**, 506 (2015).
- ³⁰S. R. White, *Phys. Rev. Lett.* **69**, 2863 (1992).
- ³¹S. R. White, *Phys. Rev. B* **48**, 10345 (1993).
- ³²U. Schollwöck, *Rev. Mod. Phys.* **77**, 259 (2005).
- ³³U. Schollwöck, *Ann. Phys.* **326**, 96 (2011).
- ³⁴Ö. Legeza, R. M. Noack, J. Solyom, and L. Tincani, in *Computational Many-Particle Physics*, Lecture Notes in Physics, Vol. 739, edited by H. Fehske, R. Schneider, and A. Weisse (2008) pp. 653–664.

- ³⁵G. K.-L. Chan, J. J. Dorando, D. Ghosh, J. Hachmann, E. Neuscamman, H. Wang, and T. Yanai, in *Frontiers in Quantum Systems in Chemistry and Physics*, Progress in Theoretical Chemistry and Physics, edited by S. Wilson, P. J. Grout, J. Maruani, G. Delgado-Barrio, and P. Piecuch (Springer Netherlands, 2008) pp. 49–65.
- ³⁶K. H. Marti and M. Reiher, *Z. Phys. Chem.* **224**, 583 (2010).
- ³⁷K. H. Marti and M. Reiher, *Phys. Chem. Chem. Phys.* **13**, 6750 (2011).
- ³⁸G. K.-L. Chan and S. Sharma, *Annu. Rev. Phys. Chem.* **62**, 465 (2011).
- ³⁹S. Wouters and D. van Neck, *Eur. Phys. J. D* **68**, 272 (2014).
- ⁴⁰Y. Kurashige, *Mol. Phys.* **112**, 1485 (2014).
- ⁴¹T. Yanai, Y. Kurashige, W. Mizukami, J. Chalupsky, T. N. Lan, and M. Saitow, *Int. J. Quantum Chem.* **115**, 283 (2015).
- ⁴²S. Szalay, M. Pfeffer, V. Murg, G. Barcza, F. Verstraete, R. Schneider, and Ö. Legeza, *Int. J. Quantum Chem.* **115**, 1342 (2015).
- ⁴³S. Knecht, E. D. Hedegård, S. Keller, A. Kovyrshin, Y. Ma, A. Muolo, C. J. Stein, and M. Reiher, *Chimia* **70**, 244 (2016).
- ⁴⁴G. K.-L. Chan, A. Keselman, N. Nakatani, Z. Li, and S. R. White, *J. Chem. Phys.* **145**, 014102 (2016).
- ⁴⁵D. Zgid and M. Nooijen, *J. Chem. Phys.* **128**, 144116 (2008).
- ⁴⁶D. Ghosh, J. Hachmann, T. Yanai, and G. K.-L. Chan, *J. Chem. Phys.* **128**, 144117 (2008).
- ⁴⁷S. Knecht, O. Legeza, and M. Reiher, *J. Chem. Phys.* **140**, 041101 (2014).
- ⁴⁸P.-A. Malmqvist and B. O. Roos, *Chem. Phys. Lett.* **155**, 189 (1989).
- ⁴⁹P.-A. Malmqvist, *Int. J. Quantum Chem.* **30**, 479 (1986).
- ⁵⁰J. Olsen, M. R. Godefroid, P. Jönsson, P.-A. Malmqvist, and C. F. Fischer, *Phys. Rev. E* **52**, 4499 (1995).
- ⁵¹J. Olsen, *J. Chem. Phys.* **143**, 114102 (2015).
- ⁵²Z. Chen, X. Chen, and W. Wu, *J. Chem. Phys.* **138**, 164120 (2013).
- ⁵³J. Olsen, B. O. Roos, P. Jørgensen, and H. J. A. Jensen, *J. Chem. Phys.* **89**, 2185 (1988).
- ⁵⁴B. O. Roos, in *Lecture Notes in Quantum Chemistry: European Summer School in Quantum Chemistry*, edited by B. O. Roos (Springer Verlag, Berlin Heidelberg, 1992) pp. 177–254.

- ⁵⁵B. O. Roos, in *Radiation Induced Molecular Phenomena in Nucleic Acids*, edited by M. K. Shukla and J. Leszczynski (Springer, 2008) pp. 125–156.
- ⁵⁶S. Keller, M. Dolfi, M. Troyer, and M. Reiher, *J. Chem. Phys.* **143**, 244118 (2015).
- ⁵⁷S. Keller and M. Reiher, *J. Chem. Phys.* **144**, 134101 (2016).
- ⁵⁸M. Moshinsky and T. H. Seligman, *Ann. Phys.* **66**, 311 (1971).
- ⁵⁹T. Helgaker, P. Jørgensen, and J. Olsen, eds., *Molecular Electronic-Structure Theory*, 1st ed. (Wiley & Sons, Chichester (England), 2000).
- ⁶⁰P.-O. Löwdin, *J. Chem. Phys.* **18**, 365 (1950).
- ⁶¹W. Heitler and F. London, *Z. Phys.* **44**, 455 (1927).
- ⁶²P. Löwdin, *J. Mol. Struct. (Theochem)* **229**, 1 (1991).
- ⁶³W. Wu, P. Su, S. Shaik, and P. C. Hiberty, *Chem. Rev.* **111**, 7557–7593 (2011).
- ⁶⁴Z. Rashid and J. H. van Lenthe, *J. Chem. Phys.* **138**, 054105 (2013).
- ⁶⁵Z. Chen, X. Chen, and W. Wu, *J. Chem. Phys.* **138**, 164119 (2013).
- ⁶⁶A. J. W. Thom and M. Head-Gordon, *J. Chem. Phys.* **131**, 124113 (2009).
- ⁶⁷E. J. Sundstrom and M. Head-Gordon, *J. Chem. Phys.* **140**, 114103 (2014).
- ⁶⁸P.-O. Löwdin, *Phys. Rev.* **97**, 1474 (1955).
- ⁶⁹F. Prosser and S. Hagstrom, *Int. J. Quantum Chem.* **2**, 89 (1968).
- ⁷⁰E. E. Weltin, *Int. J. Quantum Chem.* **10**, 163 (1976).
- ⁷¹E. Dalgaard, *Theoret. Chim. Acta* **64**, 181 (1983).
- ⁷²J. Verbeek and J. H. van Lenthe, *Int. J. Quantum Chem.* **40**, 201 (1991).
- ⁷³J. Verbeek and J. H. van Lenthe, *J. Mol. Struct: Theochem* **229**, 115 (1991).
- ⁷⁴H. Koch and E. Dalgaard, *Chem. Phys. Lett.* **212**, 193 (1993).
- ⁷⁵C. Amovilli, in *Quantum Systems in Quantum Chemistry and Physics*, edited by R. McWeeny, J. Maruani, Y. G. Smeyers, and S. Wilson (Kluwer Academic Publishers, 1997) pp. 343–347.
- ⁷⁶F. Dijkstra and J. H. van Lenthe, *Int. J. Quantum Chem.* **67**, 77 (1998).
- ⁷⁷J. Slater, *Phys. Rev.* **34**, 1293 (1929).
- ⁷⁸E. Condon, *Phys. Rev.* **36**, 1121 (1930).
- ⁷⁹J. J. W. McDouall, *Theor. Chim. Acta* **83**, 339 (1992).
- ⁸⁰P.-A. Malmqvist, B. O. Roos, and B. Schimmelpfennig, *Chem. Phys. Lett.* **357**, 230 (2002).
- ⁸¹P. Jordan and E. Wigner, *Z. Phys.* **47**, 631 (1928).

- ⁸²F. Aquilante, J. Autschbach, R. K. Carlson, L. F. Chibotaru, M. G. Delcey, L. De Vico, I. Fdez. Galván, N. Ferré, L. M. Frutos, L. Gagliardi, M. Garavelli, A. Giussani, C. E. Hoyer, G. Li Manni, H. Lischka, D. Ma, P. Å. Malmqvist, T. Müller, A. Nenov, M. Olivucci, T. B. Pedersen, D. Peng, F. Plasser, B. Pritchard, M. Reiher, I. Rivalta, I. Schapiro, J. Segarra-Martí, M. Stenrup, D. G. Truhlar, L. Ungur, A. Valentini, S. Vancoillie, V. Veryazov, V. P. Vysotskiy, O. Weingart, F. Zapata, and R. Lindh, *J. Comp. Chem.* **37**, 506 (2015).
- ⁸³M. Douglas and N. M. Kroll, *Ann. Phys.* **82**, 89 (1974).
- ⁸⁴B. A. Hess, *Phys. Rev. A* **33**, 3742 (1986).
- ⁸⁵M. Reiher, *Theor. Chem. Acc.* **116**, 241 (2006).
- ⁸⁶H. J. Aa. Jensen, oral presentation given at the REHE conference in Mühlheim (Germany), 2005.
- ⁸⁷W. Kutzelnigg and W. Liu, *J. Chem. Phys.* **123**, 241102 (2005).
- ⁸⁸T. Saue, *ChemPhysChem* **12**, 3077 (2011).
- ⁸⁹D. Peng and M. Reiher, *Theor. Chem. Acc.* **131**, 3 (2012).
- ⁹⁰B. A. Heß, C. M. Marian, U. Wahlgren, and O. Gropen, *Chem. Phys. Lett.* **251**, 365 (1996).
- ⁹¹J. Tatchen and C. M. Marian, *Chem. Phys. Lett.* **313**, 351 (1999).
- ⁹²B. Schimmelpfennig, AMFI is an atomic mean-field spin-orbit integral program, University of Stockholm, 1996.
- ⁹³M. E. Rose, *Elementary Theory of Angular Momentum* (Dover Publications, 1995).
- ⁹⁴Y. Kurashige and T. Yanai, *J. Chem. Phys.* **135**, 094104 (2011).
- ⁹⁵Y. Kurashige, J. Chalupsky, T. N. Lan, and T. Yanai, *J. Chem. Phys.* **141**, 174111 (2014).
- ⁹⁶S. Wouters, V. Van Speybroeck, and D. Van Neck, *J. Chem. Phys.* **145**, 054120 (2016).
- ⁹⁷S. Sharma and G. K.-L. Chan, *J. Chem. Phys.* **141**, 111101 (2014).
- ⁹⁸A. Y. Sokolov and G. K.-L. Chan, *J. Chem. Phys.* **144**, 064102 (2016).
- ⁹⁹M. Roemelt, S. Guo, and G. K.-L. Chan, *J. Chem. Phys.* **144**, 204113 (2016).
- ¹⁰⁰S. Guo, M. A. Watson, W. Hu, Q. Sun, and G. K.-L. Chan, *J. Chem. Theory Comput.* **12**, 1583 (2016).
- ¹⁰¹L. Freitag, S. Knecht, C. Angeli, and M. Reiher, *J. Chem. Theory Comput.* (2016), submitted, arXiv:1608.02006.

- ¹⁰²J.-B. Rota, S. Knecht, T. Fleig, D. Ganyushin, T. Saue, F. Neese, and H. Bolvin, J. Chem. Phys. **135**, 114106 (2011).
- ¹⁰³B. O. Roos, R. Lindh, P.-Å. Malmqvist, V. Veryazov, and P.-O. Widmark, J. Phys. Chem. A **108**, 2851 (2004).
- ¹⁰⁴B. O. Roos, R. Lindh, P.-Å. Malmqvist, V. Veryazov, and P.-O. Widmark, Chem. Phys. Lett. **409**, 295 (2005).
- ¹⁰⁵A. Wolf, M. Reiher, and B. A. Hess, J. Chem. Phys. **117**, 9215 (2002).
- ¹⁰⁶K. P. Huber and G. Herzberg, *Molecular Spectra and Molecular Structure: Constants of Diatomic Molecules* (Van Nostrand Reinhold, New York, 1979).
- ¹⁰⁷F. Gendron, B. Pritchard, H. Bolvin, and J. Autschbach, Inorg. Chem. **53**, 8577 (2014).
- ¹⁰⁸T. H. Dunning Jr., J. Chem. Phys. **90**, 1007 (1989).
- ¹⁰⁹K. G. Dyall, Theor. Chem. Acc. **117**, 491 (2007).